

## Shape functions of dipolar ferromagnets at and above the Curie point

E. Frey, F. Schwabl, and S. Thoma

*Institut für Theoretische Physik, Physik-Department der Technischen Universität München,  
D-8046 Garching, Federal Republic of Germany*

(Received 8 March 1989)

The critical dynamics of dipolar ferromagnets are investigated by a mode-coupling theory. The dynamical scaling functions for the Kubo relaxation functions and the damping coefficients are computed. The shape of the transverse scaling functions shows a crossover at the dipolar wave vector  $q_D$ , while the characteristic time has its crossover at about a tenth of  $q_D$ . For wave vectors smaller than  $q_D$  the critical transverse correlation function decays nearly exponentially with time. On the basis of this theory, we interpret neutron scattering experiments (constant-wave-vector and constant-energy scans) on EuO, EuS, and Fe. The agreement of the theory can be extended beyond the immediate vicinity of the critical point by including van Hove terms in the damping coefficients.

### I. INTRODUCTION

The critical dynamics of ferromagnets has been a matter of debate over many years both theoretically and experimentally. There are a variety of experimental methods, each sampling different regions of wave-vector space. These measurements indicate that the critical dynamics of isotropic ferromagnets cannot be explained solely on the basis of the short-range exchange interaction. In hyperfine-interaction (HFI) experiments on Fe and Ni, one observes a crossover in the dynamical critical exponent from  $z = \frac{5}{2}$  to  $z = 2$ ;<sup>1-4</sup> i.e., a crossover to a dynamics with a nonconserved order parameter. This is confirmed by electron-spin-resonance (ESR) and magnetic relaxation experiments,<sup>5-10</sup> where one finds a nonvanishing Onsager coefficient at zero wave vector. However, in contrast a critical exponent  $z = \frac{5}{2}$  is deduced from the wave-vector dependence of the linewidth observed in neutron scattering experiments right at the critical temperature.<sup>11-21</sup> Nevertheless, the data for the linewidths above the transition temperature<sup>13,14,22</sup> cannot be described by the Resibois-Piette scaling function resulting from a mode-coupling (MC) theory<sup>23</sup> and a renormalization-group (RG) theory,<sup>24,25</sup> which take into account the short-range exchange interaction only. Those apparent experimental discrepancies were resolved recently by a MC theory,<sup>26,27</sup> which on top of the exchange interaction, takes into account the dipole-dipole interaction present in all real ferromagnets.

Another important problem is the shape of the correlation functions. For the short-range exchange interaction this problem was analyzed by means of a discrete version of MC theory in Refs. 28-31, and by a RG theory in Refs. 32 and 33. All these theories fail to reproduce the nearly exponential decay of the Kubo function, found by spin-echo experiments on EuO at  $q = 0.024 \text{ \AA}^{-1}$  and  $T = T_c$ .<sup>15</sup> Only at larger wave vectors are the RG and MC calculations in accord with the experiment, as shown by a comparison<sup>34</sup> of the shape of the RG theory<sup>32,33</sup> with the heuristic shape of Ref. 18. The discrete versions of

the MC theory give a quite reasonable agreement with experiments for large wave vectors near the Brillouin-zone boundary, as can be inferred from Ref. 31. It was argued in Refs. 35 and 36 that neither MC nor RG theory is valid in the time regime probed by Mezei's<sup>15</sup> experiments. To fit the experimental results a "hybrid theory"<sup>36</sup> was proposed, which is a phenomenological interpolation scheme between the short- and long-time limits. In contrast we have shown in a brief report<sup>37</sup> that the experiment can be explained naturally within our dipolar MC theory without any need for a special treatment of the short-time behavior.

Certain features of the shape of the correlation function can be accentuated by constant energy scans. The RG theory (based on the short-range exchange interaction) predicts a flat curve for the reduced peak position  $q_0 \omega^{-5/2}$  plotted versus the scaled frequency  $\omega \xi^{5/2}$ .<sup>38,25</sup> In certain energy and wave-vector regions, this theoretical result is confirmed experimentally.<sup>20</sup> However, recently Böni *et al.*<sup>22</sup> have found pronounced departures from the isotropic results in EuS in a region, where according to Refs. 26 and 27, the dipolar interaction should have a considerable effect on the dynamics. This is quite similar to the situation in constant wave-vector scans, where one finds deviations from the Resibois-Piette scaling function.<sup>13,14</sup> We will give an explanation of these anomalies on the basis of the MC theory including the long-range dipolar forces.

At first sight it may be surprising that the relatively weak dipolar interaction is responsible for the anomalies observed in the critical dynamics. However, the dipolar interaction has the following characteristic features, which have important consequences on the critical dynamics. (1) In contrast to the short-range exchange interaction, the dipolar interaction is of long range and thus dominates the asymptotic critical behavior of ferromagnets. (2) It introduces an anisotropy of the spin fluctuations longitudinal and transverse to the wave vector  $\mathbf{q}$ . This implies that the longitudinal static susceptibility remains finite for  $\mathbf{q} \rightarrow 0$  and  $T \rightarrow T_c$ .<sup>39</sup> (3) The or-

der parameter is no longer conserved, as can be inferred from the equations of motion.<sup>26,27</sup> (4) The strength of the dipolar interaction introduces, besides the correlation length  $\xi$ , a second length scale  $q_D^{-1}$ , where  $q_D$  is the so-called dipolar wave vector defined below. This leads to generalized scaling laws for the relaxation functions and the linewidths.

For later reference let us now make some remarks about the structure of MC theory. The basic idea underlying MC theory is that near the critical point the relevant dynamics are described through slowly varying macroscopic modes; i.e., the conserved quantities and the order parameter. The dynamics are formulated most conveniently in terms of the Kubo relaxation functions for the spin variables  $S^i(\mathbf{q}, t)$ , which are defined by

$$\Phi^{ij}(\mathbf{q}, t) = i \lim_{\epsilon \rightarrow 0} \int_t^\infty d\tau \epsilon^{-\epsilon} \langle [S^i(\mathbf{q}, \tau), S^j(\mathbf{q}, 0)^\dagger] \rangle, \quad (1.1)$$

with the normalization  $\Phi^{ij}(\mathbf{q}, t=0) = 1$ ; i.e., the spin variables are normalized with respect to the static susceptibilities. The corresponding frequency-dependent relaxation functions are defined by a half-sided Fourier transform

$$\Phi^{ij}(\mathbf{q}, \omega) = \int_0^\infty dt e^{i\omega t} \Phi^{ij}(\mathbf{q}, t). \quad (1.2)$$

This Kubo relaxation function is related to the transport coefficients  $\Gamma^{ij}(\mathbf{q}, t)$  and the frequency matrix  $\omega^{ij}(\mathbf{q})$  by

$$\frac{d}{dt} \Phi^{ij}(\mathbf{q}, t) = i \omega^{ik}(\mathbf{q}) \Phi^{kj}(\mathbf{q}, t) - \int_0^t d\tau \Gamma^{ik}(\mathbf{q}, t-\tau) \Phi^{kj}(\mathbf{q}, \tau), \quad (1.3)$$

where the frequency matrix is given by

$$\omega^{ij}(\mathbf{q}) = \frac{1}{[\chi^i(\mathbf{q})\chi^j(\mathbf{q})]^{1/2}} \langle [S^i(\mathbf{q}, t), S^j(-\mathbf{q}, t)] \rangle. \quad (1.4)$$

The  $\Gamma^{ik}(\mathbf{q}, t)$  are determined self-consistently from decay processes of the spin modes. If only two-mode decay processes are taken into account, the spin-relaxation functions enter quadratically into the coupled integro-differential equations for the  $\Gamma^{ik}(\mathbf{q}, t)$ . Frequently one introduces, in addition, a Lorentzian approximation for the Kubo relaxation functions, which results in a simplified set of MC equations for the linewidths. For instance the Resibois-Piette scaling function for isotropic ferromagnets is obtained on this level of approximation.

The MC equations for ferromagnets with both dipolar and exchange interaction were derived in Ref. 26. As can be inferred from Refs. 26 and 27, the linewidths can be determined satisfactorily by the Lorentzian approximation. However, in order to obtain information about the line shape, one has to refrain from this approximation and has to solve the complete set of MC equations.<sup>37</sup> Then one finds a crossover in the line shape of the transverse Kubo function from a shape similar to that found in RG calculations<sup>32,33</sup> at large wave vectors (i.e.,  $q \geq q_D$ ) to a Lorentzian-like shape at  $q \ll q_D$ . This explains the nearly exponential decay of the transverse Kubo function found by spin-echo experiments on EuO.<sup>15</sup> The time dependence of the longitudinal shape function is Gaussian for small times and shows an oscillatory behavior.

In this paper we expose the arguments in more detail

and present, in addition, the results for temperatures above  $T_c$ . Specific predictions are made for EuO, EuS, and Fe. Furthermore, we examine the influence of van Hove terms and static irrelevant interactions on the critical dynamics. The outline of the paper is as follows: In Sec. II we formulate the MC theory for dipolar ferromagnets starting from a Hamiltonian, which contains both the short-range exchange and the long-range dipole-dipole interaction. The symmetry of this Hamiltonian leads us to introduce spin modes longitudinal and transverse with respect to the wave vector  $\mathbf{q}$ . From the MC equations we obtain generalized scaling laws for the relaxation functions and linewidths. The set of self-consistent MC equations for these scaling functions is derived. In Sec. III we present numerical results for the substances Fe, EuO, and EuS. Reference is made to particular experiments (i) spin-echo experiments, (ii) constant wave-vector scans, and (iii) constant energy scans. A comparison is made of the Lorentzian approximation with the complete theory. Section IV is devoted to an examination of the influence of van Hove terms in the transport coefficients and of static irrelevant interactions on the critical dynamics. In Sec. V we give a summary and discussion of the results.

## II. GENERAL THEORY

The spin Hamiltonian, including both short-range exchange and long-range dipolar interactions, is given by<sup>39</sup>

$$H = \int \frac{d^3q}{(2\pi)^3} [(J_0 + Jq^2)\delta^{ij} + JgD^{ij}(\mathbf{q})] S^i(\mathbf{q}) S^j(-\mathbf{q}), \quad (2.1)$$

where  $S^i(\mathbf{q})$  are the Fourier-transformed Cartesian components of the spin operator  $S^i(\mathbf{x})$

$$S^i(\mathbf{q}) = \int d^3x e^{-i\mathbf{q}\cdot\mathbf{x}} S^i(\mathbf{x}). \quad (2.2)$$

The parameters  $J_0$  and  $J$  characterize the exchange interaction, with the former not entering the equations of motion. The Fourier-transformed dipolar interaction is represented by the function

$$D^{ij}(\mathbf{q}) = \frac{q^i q^j}{q^2} + \frac{a_2}{a_1} q^i q^j + \left[ \frac{a_3}{a_1} + \frac{a_4}{a_1} q^2 - \frac{a_5}{a_1} (q^i)^2 \right] \delta^{ij}, \quad (2.3)$$

where  $a_i$  are constants depending on the lattice structure.<sup>39</sup> The ratio of dipolar to exchange interaction is characterized by the dimensionless parameter  $g$

$$g = \frac{a_1 (g_L \mu_B)^2}{2Ja^3} = (q_D a)^2, \quad (2.4)$$

which defines the dipolar wave vector  $q_D$ . Note that all quantities are given in units of the nearest-neighbor distance  $a$ . Here  $g_L$  is the Landé factor and  $\mu_B$  the Bohr magneton.

If one retains only those terms in the Hamiltonian, which are relevant in the sense of the RG theory (see also Sec. IV B), the Hamiltonian reduces to

$$H = \int \frac{d^3q}{(2\pi)^3} \left[ (J_0 + Jq^2)\delta^{ij} + Jg \frac{q^i q^j}{q^2} \right] S^i(\mathbf{q}) S^j(-\mathbf{q}) . \quad (2.5)$$

Since the dipolar interaction contains the projection operator ( $q^i q^j / q^2$ ), the static as well as the dynamic critical behavior is quite different for the spin modes longitudinal and transverse with respect to the wave vector  $\mathbf{q}$ . The static transverse susceptibility diverges with the dipolar critical exponent  $\gamma$  (Ref. 39) as the critical temperature is approached, whereas the longitudinal susceptibility remains finite. The matrix of the static susceptibility is given by

$$\chi^{ij}(g, \mathbf{q}) = \chi^T(g, q) \left[ \delta^{ij} - \frac{q^i q^j}{q^2} \right] + \chi^L(g, q) \frac{q^i q^j}{q^2} , \quad (2.6)$$

where we will use the Ornstein-Zernike forms for the longitudinal and transverse susceptibilities

$$\chi^T(g, q) = \frac{1}{J} \frac{1}{q^2 + \xi^{-2}} , \quad (2.6a)$$

$$\chi^L(g, q) = \frac{1}{J} \frac{1}{q^2 + g + \xi^{-2}} . \quad (2.6b)$$

The mode-coupling theory does not account for effects of the critical exponent  $\eta$ , which will be neglected in the following. Here

$$\xi = \xi_0 \left[ \frac{T - T_c}{T_c} \right]^{-\nu}$$

is the correlation length. The static crossover from Heisenberg to dipolar critical behavior is partly contained in  $\xi$  through the effective exponent  $\nu \cong \gamma_{\text{eff}}/2$ .<sup>40,41</sup>

The tensorial structure of the static susceptibility sug-

gests a decomposition of the spin operator  $\mathbf{S}(\mathbf{q})$  into one longitudinal and two transverse components with respect to the wave vector  $\mathbf{q}$ ; i.e.,

$$\mathbf{S}(\mathbf{q}) = S^L(\mathbf{q})\hat{\mathbf{q}} + S^{T_1}(\mathbf{q})\hat{\mathbf{t}}^1(\hat{\mathbf{q}}) + S^{T_2}(\mathbf{q})\hat{\mathbf{t}}^2(\hat{\mathbf{q}}) , \quad (2.7)$$

where the orthonormal set of unit vectors is defined by

$$\hat{\mathbf{q}} = \frac{\mathbf{q}}{q} , \quad \hat{\mathbf{t}}^1(\hat{\mathbf{q}}) = \frac{\mathbf{q} \times \mathbf{e}_3}{(q_1^2 + q_2^2)^{1/2}} , \quad \hat{\mathbf{t}}^2(\hat{\mathbf{q}}) = \hat{\mathbf{q}} \times \hat{\mathbf{t}}^1(\hat{\mathbf{q}}) . \quad (2.8)$$

For vanishing components of  $\mathbf{q}$  the limits are taken in the order of increasing Cartesian components. In the following we will use these longitudinal and transverse spin operators for the description of the dynamics. The Kubo relaxation functions of the spin variables  $S^\alpha(\mathbf{q}, t)$  are defined by ( $\alpha = L, T_1, T_2$ )

$$\Phi^\alpha(\mathbf{q}, t) = i \lim_{\epsilon \rightarrow 0} \int_t^\infty d\tau e^{-\epsilon\tau} \langle [S^\alpha(\mathbf{q}, \tau), S^\alpha(\mathbf{q}, 0)^\dagger] \rangle , \quad (2.9a)$$

with the normalization  $\Phi^\alpha(\mathbf{q}, t=0) = 1$ ; i.e., the spin variables are normalized with respect to the static susceptibilities. The corresponding frequency-dependent relaxation functions are defined by a half-sided Fourier transform

$$\Phi^\alpha(\mathbf{q}, \omega) = \int_0^\infty dt e^{i\omega t} \Phi^\alpha(\mathbf{q}, t) . \quad (2.9b)$$

From the Heisenberg equations of motion for the spin operators one derives the following set of mode-coupling equations for the damping  $\Gamma^\alpha(q, g, t)$  and relaxation functions  $\Phi^\alpha(q, g, t)$ :<sup>26,27</sup>

$$\frac{\partial}{\partial t} \Phi^\alpha(q, g, t) = - \int_0^t d\tau \Gamma^\alpha(q, g, t - \tau) \Phi^\alpha(q, g, \tau) , \quad (2.10)$$

and

$$\Gamma^\alpha(q, g, t) = 2J^2 k_B T \int_{\text{BZ}} \frac{d^3k}{(2\pi)^3} \sum_{\beta, \sigma} v_{\beta\sigma}^\alpha(k, q, g, \theta) (\delta^{\sigma, T} + \delta^{\alpha, T} \delta_{\beta, L} \delta_{\sigma, L}) \frac{\chi^\beta(k, g) \chi^\sigma(|\mathbf{q} - \mathbf{k}|, g)}{\chi^\alpha(q, g)} \Phi^\beta(k, g, t) \Phi^\sigma(|\mathbf{q} - \mathbf{k}|, g, t) . \quad (2.11)$$

Here the  $k$  integration runs over the first Brillouin zone (BZ). The vertex functions  $v_{\beta\sigma}^\alpha$  for the decay of the mode  $\alpha$  into the modes  $\beta$  and  $\sigma$  can be found in Refs. 26 and 27.

Equation (2.11) describes two-mode decay processes. As emphasized before, the dipolar interaction introduces a second length scale  $q_D^{-1}$  besides the correlation length  $\xi$ . This entails the following extension of the static scaling law:

$$\chi^\alpha(q, g) = \frac{1}{J} q^{-2} \hat{\chi}^\alpha(x, y) , \quad (2.12)$$

with the scaling variables

$$x = \frac{1}{q\xi} ,$$

and

$$(2.13)$$

$$y = \frac{\sqrt{g}}{q} .$$

Since the vertex functions  $v_{\beta\sigma}^\alpha$  are proportional to the fourth power of the wave number,  $v_{\beta\sigma}^\alpha \propto q^4$ , the dynamical scaling functions derived from Eqs. (2.10) and (2.11) obey the dynamical scaling laws

$$\Phi^\alpha(ql, gl^2, \omega l^z) = l^{-z} \Phi^\alpha(q, g, \omega) , \quad (2.14a)$$

and

$$\Gamma^\alpha(ql, gl^2, \omega l^z) = l^z \Gamma^\alpha(q, g, \omega) , \quad (2.14b)$$

with  $z = \frac{5}{2}$  and a scaling parameter  $l$ . We emphasize that despite  $z$  assuming the isotropic value  $\frac{5}{2}$ , there is a crossover to dipolar critical behavior contained in the functional form of the correlation functions. An immediate

consequence of Eq. (2.14a) is the following scaling property of the characteristic longitudinal and transverse frequencies  $\omega_c^\alpha(q, g)$ :

$$\omega_c^\alpha(q, g) = \Lambda q^z \Omega^\alpha(x, y), \quad (2.15)$$

where  $\Lambda$  is a nonuniversal coefficient.

Now there are various ways to rewrite the scaling laws [(2.14a) and (2.14b)] by appropriate choices of  $l$ . If one sets  $l = q^{-1}$  one finds,

$$\Phi^\alpha(q, g, \omega) = q^{-z} \hat{\Phi}^\alpha \left[ \frac{1}{q\xi}, \frac{g}{q^2}, \frac{\omega}{q^z} \right], \quad (2.16a)$$

and

$$\Gamma^\alpha(q, g, \omega) = q^z \hat{\Gamma}^\alpha \left[ \frac{1}{q\xi}, \frac{g}{q^2}, \frac{\omega}{q^z} \right]. \quad (2.16b)$$

A disadvantage of Eqs. (2.16a) and (2.16b) is that both the crossover of the time scales and of the shapes of the correlation functions are contained in  $\hat{\Phi}^\alpha$ . Since the time scales for the isotropic and dipolar critical and hydrodynamic behavior differ drastically, it is more natural to measure frequencies in units of the characteristic frequencies. Hence, we fix the scaling parameter by the condition

$$l^z = \frac{1}{\Lambda q^z \Omega^\alpha(x, y)},$$

and find from Eqs. (2.14a) and (2.14b),

$$\Phi^\alpha(q, g, \omega) = \frac{1}{\Lambda q^z \Omega^\alpha(x, y)} \phi^\alpha(x, y, \nu_\alpha), \quad (2.17a)$$

and

$$\Gamma^\alpha(q, g, \omega) = \Lambda q^z \Omega^\alpha(x, y) \gamma^\alpha(x, y, \nu_\alpha), \quad (2.17b)$$

with

$$\nu_\alpha = \frac{\omega}{\Lambda q^z \Omega^\alpha(x, y)}. \quad (2.18)$$

Equation (2.17a) separates the crossover of the frequency scales and the crossover of the shapes of the correlation

functions. The former is mainly contained in  $\Omega^\alpha(x, y)$  the latter in  $\phi^\alpha(x, y, \nu_\alpha)$ .

There is still some freedom in the choice of  $\omega_c^\alpha$  in Eq. (2.15); for instance, one could take the half-width at half maximum (HWHM) of the frequency-dependent Kubo functions. This, however, would require us to solve Eqs. (2.10) and (2.11) simultaneously for the time scales and the shapes of the correlation functions. Therefore, in the following we will use as characteristic frequencies the half-widths resulting from the Lorentzian approximation for the line shape, which are already known. The Lorentzian line widths obey the same scaling laws as the HWHM and have the same asymptotic (hydrodynamic, dipolar, isotropic) properties. Thus, this choice for the characteristic frequencies solely is a matter of numerical convenience and does not introduce any approximations. From the final result one can obtain the HWHM and rewrite the scaling functions in terms of these new variables.

Equations (2.17a), (2.17b), (2.13), and (2.18) imply for the Laplace-transformed quantities the scaling laws

$$\Phi^\alpha(q, g, t) = \phi^\alpha(x, y, \tau_\alpha), \quad (2.19a)$$

and

$$\Gamma^\alpha(q, g, t) = [\Lambda q^z \Omega^\alpha(x, y)]^2 \gamma^\alpha(x, y, \tau_\alpha), \quad (2.19b)$$

where the scaled time variables  $\tau_\alpha$  are given by

$$\tau_\alpha = \Lambda q^z \Omega^\alpha(x, y) t. \quad (2.20)$$

One should note that the characteristic time scales  $1/[\Lambda q^z \Omega^\alpha(x, y)]$  are different for the longitudinal and transverse modes. This is mainly due to the noncritical longitudinal static susceptibility implying that the longitudinal characteristic frequency  $\Lambda q^z \Omega^L(x, y)$  shows no critical slowing down asymptotically. In other words, for  $T = T_c$  and  $q \rightarrow 0$ , the longitudinal characteristic frequency does not tend to zero, which implies an effective dynamical critical exponent  $z_{\text{eff}}^L = 0$  in the limit  $q \rightarrow 0$ .

Inserting Eqs. (2.19a) and (2.19b) together with the static scaling law (2.12) into Eqs. (2.11) and (2.10) we find the following coupled integrodifferential equations:

$$\begin{aligned} \gamma^\alpha(x, y, \tau_\alpha) = & 2 \left[ \frac{\pi}{\Omega^\alpha(x, y)} \right]^2 \int_{-1}^{+1} d\eta \int_0^{\rho_{\text{cut}}} d\rho \rho^{-2} \sum_{\beta, \sigma} \hat{v}_{\beta\sigma}^\alpha(y, \rho, \eta) (\delta^{\sigma, T} + \delta^{\alpha, T} \delta^{\beta, L} \delta^{\sigma, L}) \frac{\hat{\chi}^\beta \left[ \frac{x}{\rho}, \frac{y}{\rho} \right] \hat{\chi}^\sigma \left[ \frac{x}{\rho_-}, \frac{y}{\rho_-} \right]}{\hat{\chi}^\alpha(x, y)} \\ & \times \phi^\beta \left[ \frac{x}{\rho}, \frac{y}{\rho}, \tau_{\alpha\beta}(x, y, \rho) \right] \phi^\sigma \left[ \frac{x}{\rho_-}, \frac{y}{\rho_-}, \tau_{\alpha\sigma}(x, y, \rho_-) \right], \end{aligned} \quad (2.21)$$

and

$$\frac{\partial}{\partial \tau_\alpha} \phi^\alpha(x, y, \tau_\alpha) = - \int_0^{\tau_\alpha} d\tau \gamma^\alpha(x, y, \tau_\alpha - \tau) \phi^\alpha(x, y, \tau), \quad (2.22)$$

connecting the scaling functions for the transport coefficients with the scaling functions for the Kubo relaxation functions. In Eq. (2.21) we introduced the notations  $\rho = k/q$ ,  $\rho_- = |\mathbf{q} - \mathbf{k}|/q$ ,  $\eta = \cos(\mathbf{q}, \mathbf{k})$ , and

$$\tau_{\alpha\beta}(x, y, \mu) = \tau_\alpha \mu^z \Omega^\beta(x/\mu, y/\mu) / \Omega^\alpha(x, y).$$

The nonuniversal frequency scale resulting from Eq. (2.15) is

$$\Lambda = a^{5/2} \left[ \frac{Jk_B T}{4\pi^4} \right]^{1/2} = \frac{g_L \mu_B}{q_D} \left[ \frac{k_B T a_1}{8\pi^4} \right]^{1/2}. \quad (2.23)$$

The critical dynamic exponent following from Eq. (2.14) equals  $z = \frac{5}{2}$ , however, as noted before, the crossover to dipolar behavior is contained in the scaling functions for the transport coefficients  $\gamma^\alpha(x, y, \tau_\alpha)$ , the scaling functions for the Kubo relaxation functions  $\phi^\alpha(x, y, \tau_\alpha)$  and the scaling functions of the characteristic frequencies  $\Omega^\alpha(x, y)$ .

The scaled vertex functions read<sup>26</sup>

$$\hat{v}_{\beta\beta}^\alpha = \left[ 2\eta^2 \delta^{\alpha,L} + (1-\eta^2) \left[ \delta^{\beta,T} + \frac{1}{2\rho_-^2} \right] \delta^{\alpha,T} \right] (\rho\eta - \frac{1}{2})^2, \quad (2.24)$$

$$\hat{v}_{LT}^\alpha = \left[ 2(1-\eta^2 \delta^{\alpha,L}) - (1-\eta^2) \left[ 1 + \frac{1}{\rho_-^2} \right] \delta^{\alpha,T} \right] \left[ \rho\eta - \frac{1}{2} + \frac{y^2}{2} \right]^2, \quad (2.25)$$

which are related to the vertex functions  $v_{\beta\sigma}^\alpha$  of Eq. (2.11) by  $v_{\beta\sigma}^\alpha = q^4 \hat{v}_{\beta\sigma}^\alpha$ . For both longitudinal and transverse modes, the dipolar interaction enters only in vertices involving decays into a longitudinal and a transverse mode, since the dipolar interaction enters the Hamiltonian only through the longitudinal modes.

Because the  $k$  integration is restricted to the Brillouin zone, the  $\rho$  integration of Eq. (2.21) contains the cutoff

$$\rho_{\text{cut}} = \frac{q_{\text{BZ}}}{q} = \frac{q_{\text{BZ}}}{q_D} y, \quad (2.26)$$

where  $q_{\text{BZ}}$  denotes the boundary of the first Brillouin zone. All other material dependent parameters are contained in the frequency scale  $\Lambda$ , Eq. (2.23). The cutoff (2.26) is important for small times, because the integrand of Eq. (2.21) is of order 1 for  $t=0$  and  $\rho \gg 1$ . Hence, for small times wave vectors near the zone boundary also contribute to the relaxation mechanism.

As explained before, we take for the characteristic frequencies the linewidths resulting from the Lorentzian approximation of the MC equations; i.e.,

$$\Omega^\alpha(x, y) = \gamma_{\text{Lor}}^\alpha(x, y). \quad (2.27)$$

The scaling functions of the Lorentzian linewidths  $\gamma_{\text{Lor}}^\alpha(x, y)$  are determined by the coupled integral equations<sup>26,27</sup>

$$\gamma_{\text{Lor}}^\alpha(x, y) = \frac{2\pi^2}{\hat{\chi}^\alpha(x, y)} \int_{-1}^{+1} d\eta \int_0^\infty d\rho \rho^{-2} \sum_\beta \sum_\sigma \hat{v}_{\beta\sigma}^\alpha(y, \rho, \eta) (\delta^{\sigma,T} + \delta^{\alpha,T} \delta^{\beta,L} \delta^{\sigma,L}) \frac{\hat{\chi}^\beta \left[ \frac{x}{\rho}, \frac{y}{\rho} \right] \hat{\chi}^\sigma \left[ \frac{x}{\rho_-}, \frac{y}{\rho_-} \right]}{\rho^{5/2} \gamma_{\text{Lor}}^\beta \left[ \frac{x}{\rho}, \frac{y}{\rho} \right] + \rho_-^{5/2} \gamma_{\text{Lor}}^\sigma \left[ \frac{x}{\rho_-}, \frac{y}{\rho_-} \right]}. \quad (2.28)$$

Using the solution of Eq. (2.28) as input we have solved the complete set of MC equations (2.21) and (2.22) for different values of  $q_{\text{BZ}}$ . Because there are three scaling variables ( $x$ ,  $y$ , and  $v_\alpha$ ) it is impossible to present here all numerical results. Instead, in the next section, we will concentrate on a limited number of temperatures and wave vectors motivated by the available experiments on the substances of primary interest EuS, EuO, and Fe.

In closing this section we give the results for the critical temperature ( $x=0$ ). We refer to EuO, characterized by  $q_D = 0.147 \text{ \AA}^{-1}$  and  $q_{\text{BZ}} = 1.06 \text{ \AA}^{-1}$ .<sup>15</sup> The transverse and the longitudinal scaling functions  $\phi^\alpha(x=0, y, \tau_\alpha)$  versus the scaling variables  $\tau_\alpha$  and  $y = q_D/q$  are shown in Figs. 1 and 2. The line shapes for the longitudinal and transverse Kubo relaxation functions differ significantly, especially for small wave vectors  $q \ll q_D$ ; i.e.,  $y \gg 1$ . Both functions drop off quadratically at  $t=0$ , as is implied by Eq. (2.22), but the transverse relaxation function obeys this behavior in a very small time domain only and

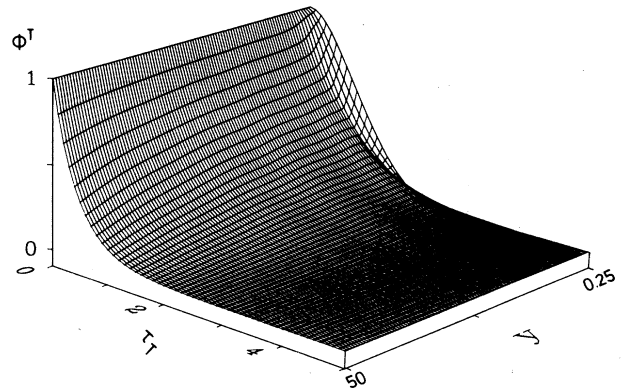


FIG. 1. Scaling function of the transverse Kubo relaxation function  $\phi^T(x=0, y, \tau_T)$  at the critical temperature vs  $\tau_T$  and  $y = q_D/q$ .

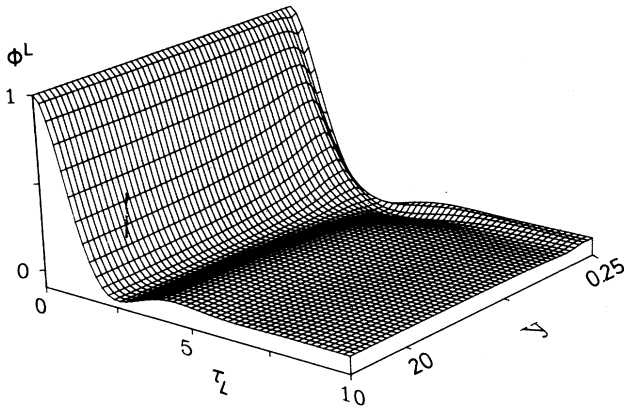


FIG. 2. Scaling function of the longitudinal Kubo relaxation function  $\phi^L(x=0, y, \tau_L)$  at the critical temperature vs  $\tau_L$  and  $y = q_D/q$ .

may be approximated best by an exponential function for  $y \gg 1$ . The longitudinal relaxation function shows a damped oscillatory behavior.

### III. APPLICATION AND PREDICTIONS FOR EXPERIMENTS

As already mentioned in Sec. II, the  $\rho$  integration in Eq. (2.21) contains a material dependent cutoff  $\rho_{\text{cut}} = yq_{\text{BZ}}/q_D$ . The ratio  $q_{\text{BZ}}/q_D$  is characteristic for the material and is collected together with other important nonuniversal parameters of EuO, EuS, and Fe in Table I.

Due to this cutoff dependence we are forced to solve Eqs. (2.21) and (2.22) for each substance separately. Nevertheless, the resulting scaling functions of the Kubo relaxation function for EuO, EuS, and Fe are nearly identical for temperatures  $T$  close to the critical temperature  $T_c$  and for small wave vectors  $q$ . This is not very surprising because of dynamic universality. The scaling functions differ in regions well separated from  $T_c$  and for wave vectors near the Brillouin-zone boundary. In the presentation of our numerical results selected according to their experimental relevance we restrict ourselves to the most important aspects.

#### A. Kubo relaxation function versus time, exemplified for EuO

In view of spin-echo experiments on EuO above  $T_c$ , the analysis of which is in progress,<sup>42</sup> we investigate the Kubo relaxation function versus time for the set of wave vectors:  $q = 0.018 \text{ \AA}^{-1}$ ,  $0.025 \text{ \AA}^{-1}$ ,  $0.036 \text{ \AA}^{-1}$ ,  $0.071 \text{ \AA}^{-1}$ ,  $0.150 \text{ \AA}^{-1}$ . In order to make evident the differences in the shape crossover for different temperatures we first examine the scaling function for the transverse and longitudinal Kubo relaxation function. In Figs. 3(a) and 3(b) these are plotted versus the scaled time variables  $\tau_\alpha$  for a temperature in the immediate vicinity of  $T_c$  ( $T = T_c + 0.25 \text{ K}$ ) and in Figs. 4(a) and 4(b) for  $T = T_c + 8 \text{ K}$ . In Fig. 3(a) one recognizes a nearly exponentially decay of the transverse scaling function for wave vectors  $q \ll q_D = 0.147 \text{ \AA}^{-1}$ . Therefore, the frequency-dependent relaxation function exhibits a Lorentzian-like shape for  $q \ll q_D$ . On the other hand for  $q \geq q_D$  the curves look similar to Gaussians for small times and oscillate for larger times. Passing from small to large wave vectors there occurs a shape crossover near the dipolar wave vector. This should be contrasted with the linewidth crossover appearing at a wave vector almost 1 order of magnitude smaller than  $q_D$  (see Refs. 26 and 27). The longitudinal scaling function in Fig. 3(b) shows a Gaussian behavior at small times and damped oscillations for larger times, which is quite different from what is found for the transverse scaling function. Furthermore, there is no crossover to an exponential decay as one passes to smaller wave vectors.

Further away from  $T_c$ , the line-shape crossover of the transverse relaxation function is much less pronounced and the shape is more Gaussian, even for wave vectors much smaller than  $q_D$ . In Figs. 4(a) and 4(b) the transverse and longitudinal Kubo functions are shown for the same wave vectors as in Figs. 3(a) and 3(b) at  $T = T_c + 8 \text{ K}$ . For this temperature the shape of the longitudinal and transverse Kubo function is nearly the same as one realizes by comparing Figs. 4(a) and 4(b). This is exactly what one would have expected, because the influence of the dipolar forces decreases with separation from the critical point and then there is no difference any more between longitudinal and transverse modes.

To single out the line-shape crossover, the appropriate time scales are  $\tau_\alpha$  of Eq. (2.20) used in Figs. 3 and 4. On

TABLE I. Material parameters for Fe, EuO, and EuS. These values are collected from Refs. 13–22 and 39.  $q_{\text{BZ}}$  is defined by replacing the simple-cubic lattice by a sphere; i.e.,  $q_{\text{BZ}} = (6\pi)^{1/3}/a$ . If there is more than one value in the literature it is given in parentheses.

	Fe	EuO	EuS
$a$ (Å)	2.87	5.12	5.95
$T_c$ (K)	1040	69.1	16.6
$q_D$ (Å <sup>-1</sup> )	0.045	0.147	0.24(0.27)
$q_{\text{BZ}}$ (Å <sup>-1</sup> )	1.7	1.06	0.66
$q_{\text{BZ}}/q_D$	38	7.5	2.8
$T_D - T_c$ (K)	8.6	8.2	4.8
$a_1$	$\sqrt{24}\pi$	$4\pi$	$4\pi$
$\Lambda_{\text{expt}}$ meV Å <sup>5/2</sup>	130	8.7(8.3)	2.1(2.25)
$\Lambda_{\text{Lor}}$ meV Å <sup>5/2</sup>	112	7.1	2.1



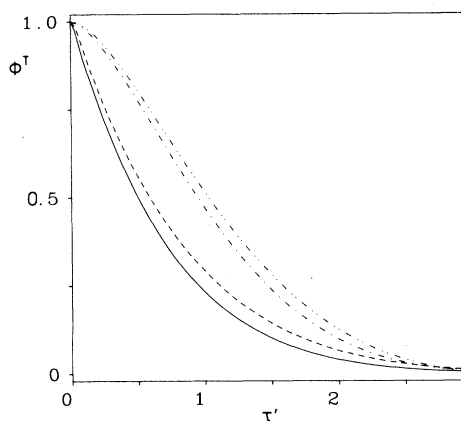


FIG. 5. Scaling function of the transverse Kubo relaxation function vs  $\tau' = \Lambda_{\text{Lor}} q^2 t$  at  $T = T_c$  for  $q = 0.025 \text{ \AA}^{-1}$  (—),  $q = 0.036 \text{ \AA}^{-1}$  (---),  $q = 0.150 \text{ \AA}^{-1}$  (-·-·-), and  $q = 0.300 \text{ \AA}^{-1}$  (- - - - -).

In order to exhibit the difference from the MC theory including only short-range exchange interaction, we have solved Eqs. (2.21) and (2.22) for this special case; i.e.,  $y = 0$ ,  $x = 0$ , and  $\rho_{\text{cut}} = q_{\text{BZ}}/q$  with  $q = 0.024 \text{ \AA}^{-1}$ . The result is the dashed curve in Fig. 7, which differs drastically from the line shape including the long-range dipolar interaction. It is important to realize that the crossover in the line shape starts nearly at  $q_D$ , whereas the linewidth still scales with the isotropic critical dynamic exponent  $z = \frac{5}{2}$  in this wave-vector region. These results have been presented already in a recent letter.<sup>37</sup> The numerical integration of the MC equations<sup>26,27</sup> was repeated in Ref. 43 leading to a confirmation of our results.

To facilitate the analysis of experiments, we give here an approximant for the transverse scaling function versus the scaled time variable  $\tau_T$

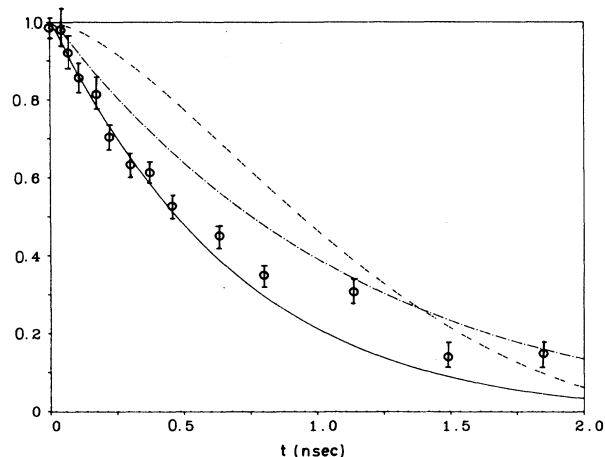


FIG. 7. Transverse Kubo relaxation function  $\Phi^T(q, g, t)$  at  $q = 0.024 \text{ \AA}^{-1}$  (—) and  $q = 0.028 \text{ \AA}^{-1}$  (-·-·-) for dipolar ferromagnets vs time in nsec. The dashed line is the Kubo relaxation function for short-range exchange interaction only at  $q = 0.024 \text{ \AA}^{-1}$ . Data points from Fig. 1 of Ref. 15.

$$\phi^T(\tau_T) = \exp \left( \frac{-\tau_T^2}{a + b\tau_T + c\tau_T^2} \right). \quad (3.1)$$

The parameters  $a$ ,  $b$ , and  $c$  are given in Table II. We have to emphasize that Eq. (3.1) is a purely numerical approximation and one should therefore refrain from a physical interpretation. The range of validity is restricted to  $y \geq 0.5$  and  $\tau_T \leq 4.5$ . This function, especially, does not show the proper exponential decrease for very large times.

Finally, let us compare the theoretical and experimental linewidths for Fe, EuO, and EuS precisely at the critical temperature. In Fig. 8 the transverse linewidth at  $T_c$

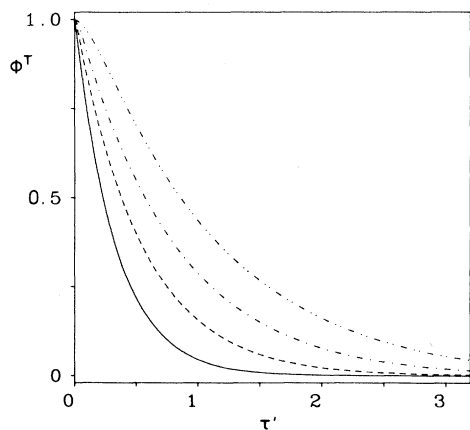


FIG. 6. Scaling function of the transverse Kubo relaxation function vs  $\tau' = \Lambda_{\text{Lor}} q^2 t$  at  $T = T_c + 0.5 \text{ K}$  for  $q = 0.018 \text{ \AA}^{-1}$  (—),  $q = 0.025 \text{ \AA}^{-1}$  (---),  $q = 0.036 \text{ \AA}^{-1}$  (-·-·-), and  $q = 0.071 \text{ \AA}^{-1}$  (- - - - -).

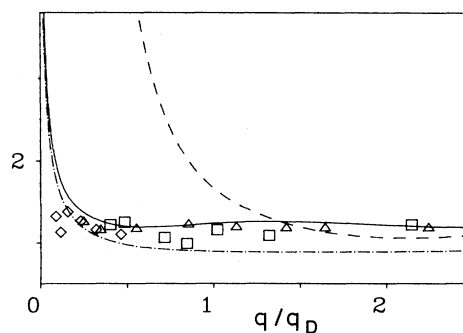


FIG. 8. Scaling functions vs  $y^{-1} = q/q_D$  at  $T_c$  (in units of the theoretical nonuniversal constant  $\Lambda$ ) for (i) the HWHM of the complete solution of the MC equations for the transverse Kubo relaxation function (—), (ii) transverse (—·—·—), and (iii) longitudinal (---) linewidth in Lorentzian approximation. Experimental data for EuO ( $\square$ ; Ref. 19,  $\diamond$ ; Ref. 14) and Fe ( $\triangle$ ; Ref. 13).

obtained in the Lorentzian approximation is compared with the HWHM resulting from the complete solution of the MC equations. Whereas these two functions are quite similar in shape, their asymptotic values differ by a factor of 1.2. The experimental data in Fig. 8 are divided by the theoretical values of the nonuniversal constants. Thus, there is agreement between experiment and the HWHM of the complete MC solution without adjustable parameters.

### C. Constant energy scans, exemplified for EuS

In conventional neutron scattering experiments one measures the scattering function  $S^T(q, \omega)$

$$S^T(q, \omega) \propto 2k_B T q^{-2} \hat{\chi}^T(x, y) F^T(q, \omega) \frac{\omega/k_B T}{1 - e^{-\omega/k_B T}}, \quad (3.2)$$

where the spectral weight function  $F^T(q, \omega)$  is related to the real part of the transverse Kubo relaxation function by

$$\begin{aligned} F^T(q, \omega) &= \text{Re}[\Phi^T(q, \omega)] \\ &= \frac{1}{\Lambda q^2 \Omega^T(x, y)} \text{Re}[\phi^T(x, y, \nu_T)]. \end{aligned} \quad (3.3)$$

A possible way of examining the line shape are constant-energy scans for the scattering function  $S^T(q, \omega)$ . Characteristic quantities in these scans are the peak position  $q_0$  and the HWHM  $\Delta q$ . For an isotropic ferromagnet the peak positions scaled by the factor  $(\Lambda/\omega)^{2/5}$  and drawn versus the scaled frequency  $\omega \xi^{5/2}/\Lambda$  should follow a single scaling function.<sup>25,38,44</sup> In constant-energy measurements above  $T_c$  for the Heisenberg ferromagnet EuS Böni *et al.*<sup>22</sup> found that the peak positions do not obey the scaling law of an isotropic ferromagnet.

One of the most striking new features introduced by the dipolar interaction is the generalized dynamical scaling Eq. (2.17) with the additional scaling variable  $y = q_D/q$ . In conventional constant  $q$  scans plotted versus the scaling variable  $x = 1/(q\xi)$ , the linewidths are not represented by a single scaling function but by a series of curves as exhibited in Fig. 3 of Ref. 26, where each curve corresponds to a fixed temperature. As noted recently<sup>37</sup> and to be shown next, the failure of the isotropic scaling law in constant-energy scans can also be attributed to the influence of the dipolar forces.

Introducing polar coordinates  $r = (x^2 + y^2)^{1/2}$  and  $\varphi = \arctan(q_D \xi)$  the generalized scaling law for the Kubo functions and characteristic frequencies leads to the following scaling law for the peak position in constant-energy scans

$$\begin{aligned} r_0 &= [(1/q_0 \xi)^2 + (q_D/q_0)^2]^{1/2}, \\ r_0 &= \mathcal{R} \left[ \varphi, \frac{\omega}{\Lambda (\xi^{-2} + q_D^2)^{z/2}} \right], \end{aligned} \quad (3.4)$$

as can be inferred easily from Eqs. (2.12) and (2.17a). This implies for  $q_0$

$$q_0 \left[ \frac{\Lambda}{\omega} \right]^{2/5} = Q \left[ \varphi, \frac{\omega}{\Lambda (\xi^{-2} + q_D^2)^{z/2}} \right]. \quad (3.5)$$

Hence if Eq. (3.5), containing the two-parameter scaling function  $Q$ , is plotted versus  $\omega \xi^{5/2}/\Lambda$  a set of curves parametrized by the scaling variable  $\varphi$  is obtained. In Fig. 9 the scaled peak position  $q_0 (\Lambda_{\text{Lor}}/\omega)^{2/5}$  is plotted versus  $\hat{\omega} = \omega \xi^{5/2}/\Lambda_{\text{Lor}}$  for the following set of scaling variables  $\varphi =$  (a) 1.490, (b) 1.294, (c) 0.970, and (d)  $\varphi = 0$ . Case (d) corresponds to an isotropic ferromagnet; i.e.,  $q_D = 0$ .  $\Lambda_{\text{Lor}}$  is related to  $\Lambda$  by  $\Lambda_{\text{Lor}} = 5.1326\Lambda$  (see also Sec. III D). The above values for  $\varphi$  correspond in the case of EuS ( $q_D = 0.27 \text{ \AA}^{-1}$ ,  $\xi_0 = 1.81 \text{ \AA}$ ) to the temperatures  $T =$  (a)  $1.01T_c$ , (b)  $1.06T_c$ , and (c)  $1.21T_c$ . Due to the generalized scaling law Eq. (3.5), the curves coincide with the isotropic theory for high frequency, but deviate for small frequency. The closer to  $T_c$  the larger the frequency, where the deviation sets in. The comparison of experiments with Fig. 9 must not be extended to arbitrary large  $\hat{\omega}$ , but has to be restricted to regions where the conditions  $\xi^{-1}$ ,  $q \ll q_{\text{BZ}}$  is met [see discussion of relation (3.8)].

The steep drop off of the scaled peak positions at particular  $\varphi$  dependent values of  $\hat{\omega}$  can be understood as follows. Because of the dipolar forces the order parameter is no more conserved. Hence, the scattering function  $S^T(q, \omega)$  remains finite for vanishing wave vector. As can be seen easily from Eq. (3.2) the frequency dependence of  $S^T(q=0, \omega)$  is given by

$$S^T(q=0, \omega) \propto \frac{\Gamma_0 \xi^2}{\omega^2 + \Gamma_0^2} \quad \text{for } T \geq T_c, \quad (3.6)$$

where  $\Gamma_0$  denotes the relaxation rate of the nonconserved order parameter in the hydrodynamic region. Since  $\Gamma_0$  is proportional to  $\xi^{-2}$  Eq. (3.6) reduces to

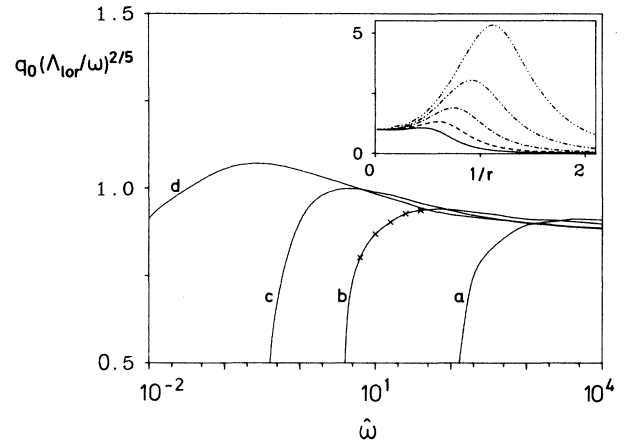


FIG. 9. Scaled peak positions  $q_0 (\Lambda_{\text{Lor}}/\omega)^{2/5}$  for constant-energy scans of the scattering function for the complete solution of the MC equations vs the scaling variable  $\hat{\omega}$  for  $\varphi =$  (a) 1.490, (b) 1.294, (c) 0.970, and (d) for the isotropic case, i.e.,  $\varphi = 0$ . Inset:  $S^T(q, \omega)/S^T(0, \omega)$  in arbitrary units vs  $1/r$  for  $\varphi = 1.294$  for some typical values of the scaled frequency [ $\hat{\omega} = 10^{L/10}$  with  $L = 8$  (—),  $10$  (---),  $12$  (-.-.-),  $14$  (-.-.-.-), and  $16$  (-.-.-.-.-) indicated in the graph by crosses].

$$S^T(q=0, \omega) \propto \frac{1}{\omega^2} \quad \text{for } T = T_c. \quad (3.7)$$

The constant-energy scans have a maximum at  $q=0$  and for sufficiently large  $\omega$  a local maximum at finite  $q$ . If  $\omega$  decreases, the former strongly increases while the latter is shifted to smaller  $q$ . As a result of this competition only the maximum at  $q=0$  survives for low frequencies. In order to substantiate this, typical constant-energy scans are shown in the inset of Fig. 9, where  $S^T(q, \omega)/S^T(0, \omega)$  (in arbitrary units) is plotted versus  $1/r$  for  $\varphi = 1.294$  and for a set of scaled frequencies ( $\hat{\omega} = 10^{L/10}$  with  $L = 8, 10, 12, 14, 16$  indicated in the graph). The corresponding scaled peak positions are indicated in the scaling plot by crosses. This behavior explains why the scaled peak positions for dipolar ferromagnets show such a steep drop off at small frequencies. We do not attempt to fit temperatures as  $2.0T_c$  by our critical theory. Due to the form of  $S^T(q, \omega)/S^T(0, \omega)$  shown in the inset of Fig. 9, we consider half-widths in constant-energy scans less significant and refrain from presenting such plots.

We further note that the characteristic deviations from the isotropic theory exhibited in Fig. 9 result from the crossover in the time scale and not so much from the crossover in the shape function. To demonstrate this, we show in Fig. 10 the scaled peak positions  $q_0(\Lambda_{\text{Lor}}/\omega)^{2/5}$  in Lorentzian approximation. Compared to Fig. 9 the maxima are overemphasized in Fig. 10, but the portions with the steep slope are nearly identical. The differences of the exact mode-coupling theory and the Lorentzian approximation can also be seen in the insets of Figs. 9 and 10.

We close this section with some remarks about the numerical procedure used in solving the MC equations in the present case. In Fig. 9 the scaled peak positions are given for fixed scaling variables  $\varphi$ . As expected, in the region of large  $\hat{\omega}$  these curves approach the isotropic result. In this limit the scaled peak positions are of the order  $O(1)$ , which implies

$$y_0 = \frac{q_D}{q_0} \approx \hat{\omega}^{-2/5} \tan \varphi. \quad (3.8)$$

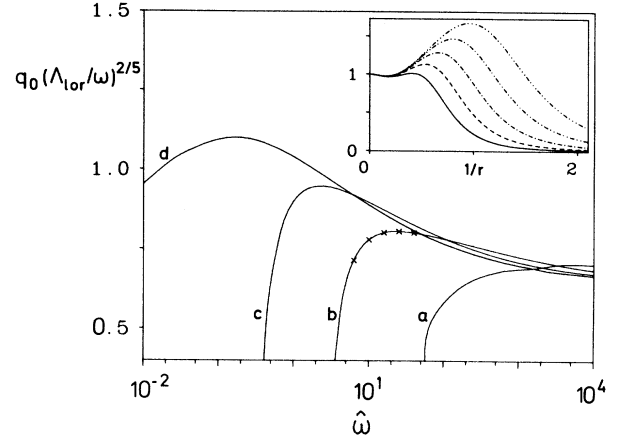


FIG. 10. The same as in Fig. 9 for the scattering function resulting from the Lorentzian approximation.

Thus  $y_0$  tends to zero for  $\hat{\omega} \rightarrow \infty$  and fixed scaling variable  $\varphi$ . By additionally fixing  $q_D$ , i.e., for a special substance, this would imply that  $q$  leaves the first Brillouin zone. There is, however, another point of view namely interpreting the limit  $y_0 \rightarrow 0$  as the fictitious limit  $q_D \rightarrow 0$ , or in other words looking at a series of different substances with decreasing relative strength of the dipolar interaction. Furthermore, the limit  $q_D \rightarrow 0$  implies  $\xi \rightarrow \infty$  for fixed  $\varphi$ , as is obvious from the definition of  $\varphi$ .

It would be tedious to solve the MC equations for a sequence of  $q_D$  with finite cutoff as in Sec. II. Instead we restrict ourselves to sufficiently small wave vectors  $q$  such that  $\rho_{\text{cut}} = q_{\text{BZ}}/q_D y = q_{\text{BZ}}/q$  may be replaced by infinity. By extending the  $\rho$  integration to infinity one has to take care of the fact that the transport coefficients  $\gamma^\alpha(x, y, \tau_\alpha)$  become singular at  $\tau_\alpha = 0$ . In order to explore the kind of singularity, let us study the behavior of the transport coefficients at very small scaled time variables. By making the substitution  $\mu = \tau_\alpha \rho^{5/2}$  in the integral of Eq. (2.21) and introducing polar coordinates  $r = (x^2 + y^2)^{1/2}$ ,  $\tan \varphi = (y/x) = q_D \xi$  one finds for  $\tau_\alpha \ll 1$ ,

$$\begin{aligned} \gamma^\alpha(r, \varphi, \tau_\alpha \ll 1) &= \frac{4}{5} \tau_\alpha^{-2/5} \left[ \frac{\pi}{\Omega^\alpha(r, \varphi)} \right]^2 \int_0^\infty d\mu \mu^{-3/5} \sum_{\beta, \sigma} \bar{v}_{\beta\sigma}^\alpha(y, \rho) \frac{\hat{\chi}^\beta(\bar{\mu}, \varphi) \hat{\chi}^\sigma(\bar{\mu}, \varphi)}{\hat{\chi}^\alpha(r, \varphi)} \\ &\quad \times \phi^\beta \left[ \bar{\mu}, \varphi, \mu \frac{\Omega^\beta(\bar{\mu}, \varphi)}{\Omega^\alpha(r, \varphi)} \right] \phi^\sigma \left[ \bar{\mu}, \varphi, \mu \frac{\Omega^\sigma(\bar{\mu}, \varphi)}{\Omega^\alpha(r, \varphi)} \right] \\ &\equiv \tau_\alpha^{-2/5} \bar{\gamma}^\alpha(r, \varphi, \tau_\alpha), \end{aligned} \quad (3.9)$$

where  $\bar{\mu} = r(\tau_\alpha/\mu)^{2/5}$  and the nonzero vertex functions  $\bar{v}_{\beta\sigma}^\alpha(y, \rho)$  are given by

$$\bar{v}_{TT}^T(y, \rho) = \frac{4}{5}, \quad (3.10a)$$

$$\bar{v}_{LT}^L(y, \rho) = \frac{8}{5} + \frac{2y^4}{3\rho^2}, \quad (3.10b)$$

$$\bar{v}_{TT}^T(y, \rho) = \frac{4}{15}, \quad (3.10c)$$

$$\bar{v}_{LT}^T(y, \rho) = \frac{16}{15} + \frac{2y^4}{3\rho^2}. \quad (3.10d)$$

Hence, for small times the transport coefficients are a product of a singular part  $\tau_\alpha^{-2/5}$  and a part  $\bar{\gamma}^\alpha(r, \varphi, \tau_\alpha)$ , which is finite for  $\tau_\alpha \rightarrow 0$ . One should note that this singular behavior is only due to the isotropic terms in the vertex functions, whereas the dipolar term  $y^4/\rho^2$  leads to

a regular time dependence. In the presence of a cutoff the singularity is absent and  $\tau_\alpha^{-2/5}$  is replaced by a constant for times smaller than a microscopic time  $t_{\text{micro}} = (\mathcal{D}q_{\text{BZ}}^2)^{-1}$ ,<sup>45</sup> where  $\mathcal{D}$  is the diffusion constant at  $q_{\text{BZ}}$ . We have incorporated these analytical results in the procedure for solving the MC equations with infinite cutoff.

#### D. Comparison of the HWHM with the Lorentzian linewidth, exemplified for Fe

In this subsection we compare the HWHM of the Kubo functions resulting from Eqs. (2.21) and (2.22) to  $\gamma_{\text{Lor}}^\alpha$  determined by Eq. (2.28). The solid lines in Fig. 11 represent the scaling functions  $\gamma_{\text{Lor}}^T(x, y)$  for the transverse linewidth in Lorentzian approximation,<sup>26,27</sup> where the curves are normalized with respect to their value at criticality

$$\gamma_{\text{Lor}}^T(x=0, y=0) = 5.1326.$$

In the case of Fe curves *a*, *b*, *c*, and *d* correspond to the temperatures  $T - T_c = 1.4, 5.8, 21.0,$  and  $51.0$  K. The nonuniversal frequency scale is then found to be  $\Lambda_{\text{Lor}} = 5.1326\Lambda = 107.2 \text{ meV \AA}^{5/2}$ , whereas the experimental value is

$$\Lambda_{\text{expt}} = 130 \text{ meV \AA}^{5/2}.$$

Now we return to the solution of the complete set of MC equations (2.21) and (2.22). The HWHM  $\Gamma_{\text{HW}}^T(q)$  for

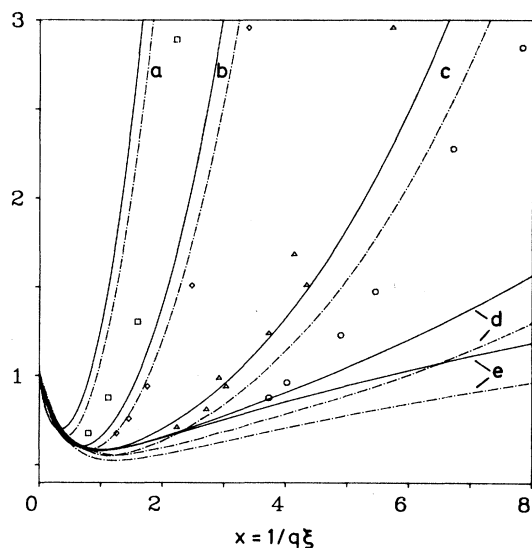


FIG. 11. Scaling function of the transverse linewidth in Lorentzian approximation (—) and of the HWHM of the complete solution (— · — · —) vs the scaling variable  $x = (q\xi)^{-1}$  for a set of temperatures [ $T - T_c =$  (a) 1.4 K, (b) 5.8 K, (c) 21 K, and (d) 51 K]. The Resibois-Piette function (—) and the HWHM from the complete solution of the MC equations (— · — · —) without dipolar interaction is also plotted (e). Experimental results for Fe from Refs. 13 and 14 [ $T - T_c =$  (□) 1.4 K, (◇) 5.8 K, (△) 21.0 K, (○) 51.0 K].

the real part of Laplace transformed transverse Kubo functions is defined by

$$\text{Re}[\Phi^T(\omega = \Gamma_{\text{HW}}^T)] = \frac{1}{2} \text{Re}[\Phi(\omega = 0)], \quad (3.11)$$

and obeys the scaling law

$$\Gamma_{\text{HW}}^T(q) = \Lambda_{\text{HW}} q^z \gamma_{\text{HW}}^T(x, y). \quad (3.12)$$

In Fig. 11 the scaling function  $\gamma_{\text{HW}}^T(x, y)$  (dashed-dotted line) is plotted for the same temperatures. The scaling function is normalized such that  $\gamma_{\text{HW}}^T(x=0, y=0) = 1$ , which gives for the nonuniversal frequency scale

$$\Lambda_{\text{HW}} = 1.37\Lambda_{\text{Lor}} = 147 \text{ meV \AA}^{5/2},$$

a value which is in reasonable agreement with experiment. The Lorentzian linewidth and the HWHM have nearly the same  $(q\xi)^{-1}$  dependence. Especially for small wave vectors, the difference comes about only because of the different nonuniversal frequency scales. Figure 11 is in accord with Fig. 4 of Ref. 43.

In spin-echo experiments on Fe (Refs. 13 and 14) the transverse Kubo relaxation function versus time  $t$  has been measured for the above temperatures. From these the linewidth  $\Gamma_{\text{expt}}^T$  was extracted by fitting the observed data with an exponential function  $\exp[-\Gamma_{\text{expt}}^T(q)t]$ . The corresponding scaled linewidths are also shown in Fig. 11. For a detailed analysis of such spin-echo experiments it would be recommendable to reanalyze the experimental data with the shape functions calculated in this article. Furthermore, the experimental definition of the linewidth does not correspond to the definition of the HWHM of the real part of the Laplace transformed Kubo function. Therefore, the comparison of theory and experiment is preliminary.

As can be inferred from Fig. 11 the complete solution of the mode-coupling theory is in reasonable agreement with the experiment close to  $T_c$  ( $T - T_c = 1.4$  and  $5.8$  K) and gives an improvement over the Lorentzian approximation. The minor differences may be due to the following reasons. (i) As mentioned above, the measured scaling functions of the transverse relaxation function were fitted to an exponential line, which is not the correct shape. (ii) Because the dipolar crossover temperature  $T_D$  of Fe is 8.6 K, static crossover effects not taken into account in the experiments may cause some changes. Furthermore, the nonuniversal scale of the correlation length  $\xi_0$  is affected by experimental uncertainties. A change in  $\xi_0$  would lead to a horizontal shift of the data points in Fig. 11.

Larger differences show up for temperatures more separated from  $T_c$  ( $T - T_c = 21$  and  $51$  K), which cannot be accounted for by the shape crossover or static crossover effects. Here the measured linewidths are larger than the theoretical. In order to explain this, it is necessary to take into account the van Hove terms and further relaxation mechanisms due to irrelevant interactions, which nevertheless may play an important role for temperatures well separated from  $T_c$  (see Sec. IV).

#### IV. INFLUENCE OF VAN HOVE TERMS AND STATIC IRRELEVANT INTERACTIONS

##### A. The influence of van Hove terms on the critical dynamics

In this section we study the influence of van Hove terms on the critical dynamics. In the early history of critical dynamics it was believed that the Onsager coefficients  $L^\alpha(q)$  would be uncritical and that the critical slowing down of the transport coefficients  $H^\alpha(q, g, t)$  would result solely from their inverse dependence on the static susceptibilities; i.e.,

$$H^\alpha(q, g, t) = \frac{L^\alpha(q)}{\chi^\alpha(q, g)} \delta(t). \quad (4.1)$$

Contributions to the transport coefficients of that type are called van Hove terms. Such contributions are always present and are generated by fast fluctuations,<sup>46-49</sup> which originate from additional irrelevant terms in the Hamiltonian and from higher-order decay processes contained in the Hamiltonian (2.5). By including the van Hove term (4.1), Eq. (2.10) remains unchanged while Eq. (2.11) is replaced by

$$\begin{aligned} \Gamma^\alpha(q, g, t) = & H^\alpha(q, g, t) + 2J^2 k_B T \int_{\text{BZ}} \frac{d^3k}{(2\pi)^3} \sum_{\beta, \sigma} v_{\beta\sigma}^\alpha(k, q, g, \theta) (\delta^{\sigma, T} + \delta^{\alpha, T} \delta^{\beta, L} \delta^{\sigma, L}) \\ & \times \frac{\chi^\beta(k, g) \chi^\sigma(|\mathbf{q}-\mathbf{k}|, g)}{\chi^\alpha(q, g)} \Phi^\beta(k, g, t) \Phi^\sigma(|\mathbf{q}-\mathbf{k}|, g, t), \end{aligned} \quad (4.2)$$

where the second term on the right-hand side is the mode-coupling term of Eq. (2.11). Retaining only the first term in the transport coefficients would result in the van Hove theory for the critical dynamics. However, close to  $T_c$  the van Hove term is small compared to the mode-coupling contribution and Eq. (4.2) reduces to Eq. (2.11).

Due to the dipolar interaction the order parameter is no longer conserved; hence, the Onsager coefficient  $L(q)$  is a finite constant  $L$  independent of  $q$ , whereas for a conserved order parameter one would have  $L(q) = Lq^2$ . From Eqs. (2.10) and (4.2) one finds MC equations for the scaling functions, which are given by (2.22) and

$$\begin{aligned} \gamma^\alpha(x, y, \tau_\alpha) = & h y^{z-2} \frac{1}{\hat{\chi}^\alpha(x, y) \Omega^\alpha(x, y)} \delta(\tau_\alpha) \\ & + 2 \left[ \frac{\pi}{\Omega^\alpha(x, y)} \right]^2 \int_{-1}^{+1} d\eta \int_0^{\rho_{\text{cut}}} d\rho \rho^{-2} \sum_{\beta, \sigma} \hat{v}_{\beta\sigma}^\alpha(y, \rho, \eta) (\delta^{\sigma, T} + \delta^{\alpha, T} \delta^{\beta, L} \delta^{\sigma, L}) \\ & \times \frac{\hat{\chi}^\beta \left[ \frac{x}{\rho}, \frac{y}{\rho} \right] \hat{\chi}^\sigma \left[ \frac{x}{\rho_-}, \frac{y}{\rho_-} \right]}{\hat{\chi}^\alpha(x, y)} \\ & \times \phi^\beta \left[ \frac{x}{\rho}, \frac{y}{\rho}, \tau_{\alpha\beta}(x, y, \rho) \right] \phi^\sigma \left[ \frac{x}{\rho_-}, \frac{y}{\rho_-}, \tau_{\alpha\sigma}(x, y, \rho_-) \right], \end{aligned} \quad (4.3)$$

where

$$h = \frac{L}{\Lambda q_D^z}. \quad (4.4)$$

Taking typical background values for  $L$  from ESR experiments<sup>10</sup>  $h$  is found to be of the order  $h = 0.05, \dots, 0.1$ . We have solved Eqs. (2.22) and (4.3) for  $h = 0.1$ . The resulting scaling functions for the transverse linewidth with (dashed-dotted) and without (solid) the van Hove term are displayed in Fig. 12. In the case of Fe ( $q_D = 0.045 \text{ \AA}^{-1}$ ,  $\xi_0 = 0.82 \text{ \AA}$ ) the set of curves correspond to the temperatures  $T - T_c = 1.4, 5.8, 21.0,$  and  $51.0 \text{ K}$ . The van Hove terms lead to an increase of the linewidths proportional to its strength  $h$ . As the critical temperature is approached the influence of the van Hove terms decreases. Furthermore, we note that the linewidth resulting from Eqs. (2.22) and (4.3) is almost the same as if one simply would have added the van Hove linewidth

$$\frac{h}{5.1326} \frac{y^{1/2}}{\hat{\chi}^\alpha(x, y)} \quad (4.5)$$

to the self-consistent solution of the MC equations

without the van Hove term, Eq. (2.21). The latter is represented by the dotted curve in Fig. 12. In Fig. 12 we have also displayed the experimental data of Mezel<sup>13,14</sup> on Fe. Close to  $T_c$  ( $T - T_c = 1.4$  and  $5.8 \text{ K}$ ) the van Hove terms are negligible. But for larger temperatures ( $T - T_c = 21.0$  and  $51.0 \text{ K}$ ) the van Hove terms drastically increase the linewidth. As can be inferred from Fig. 12 we are able to give a good description of the experimental data with quite reasonable a value of  $h = 0.1$ . The minor discrepancies remaining closer to  $T_c$  we have commented on in Sec. III C. We recall that changes in the critical exponent  $\nu$  and in  $\xi_0$  lead to horizontal shifts of the data points.

Let us finally add a comment on the magnitude of and on the role played by the van Hove terms. Their contribution to the linewidth can be regarded as a background contribution. In order to substantiate this point of view let us look at ESR experiments, for which one is able to determine the Onsager coefficient at zero wave vector. In analyzing those experiments one subtracts from the data a temperature-independent background term  $L_{\text{bg}}$ .<sup>10</sup> The remaining critical part of the Onsager coefficient shows a

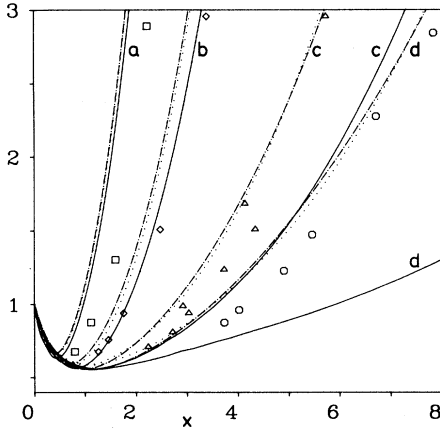


FIG. 12. Scaling function of the transverse linewidth resulting from the solution of the complete mode-coupling equations neglecting (—) and having regard of the van Hove term with  $h=0.1$  (· · · · ·) vs the scaling variable  $x=(q\xi)^{-1}$  for a set of temperatures [ $T-T_c =$  (a) 1.4 K, (b) 5.8 K, (c) 21 K, (d) 51 K]. Experimental data on Fe (Refs. 13 and 14) as in Fig. 11. The dotted curves are obtained if one simply adds the van Hove term to the self-consistent solution of the MC equations (see the text).

temperature dependence, which is very well described within our MC theory (see Refs. 27, 50, and 10). It is natural to identify this background value  $L_{bg}$  with the above defined Onsager coefficient  $L$  entering the van Hove term [Eq. (4.1)]. If one compares neutron scattering data for the linewidth with the critical theory (Fig. 11) one should also subtract such background terms from the data. Otherwise, one has to compare with a theory containing such terms (Fig. 12). Similar precautions have to be taken if one compares results from neutron scattering and ESR measurements.

### B. The influence of terms irrelevant for the statics on the critical dynamics

In this section we will analyze whether static irrelevant interactions can be incorporated into the MC approach and how the critical dynamics are affected. To start with we give a brief definition of the item irrelevant in the context of Wilson's  $q$  space RG procedure.

The renormalization-group transformation<sup>51</sup>  $H' = \mathcal{R}_b H$  is defined by integrating out the spin components  $S_q^\alpha$  with  $\Lambda/b \leq q \leq \Lambda$  followed by a rescaling of the wave vector  $q \rightarrow bq$  and spin  $S_q^\alpha \rightarrow \zeta_b S_q^\alpha$ . Here  $b$  ( $b > 1$ ),  $\zeta_b$  are rescaling parameters and  $\Lambda$  is the cutoff in  $q$  space. The transformed Hamiltonian then is given by

$$\exp(\mathcal{R}_b H) = \left[ \prod_{\alpha} \prod_{\Lambda/b \leq q' \leq \Lambda} \int dS_{q'}^\alpha \exp(H) \right]_{S_q^\alpha \rightarrow \zeta_b S_q^\alpha} \quad (4.6)$$

This transformation implies a scale transformation for the coupling constants  $\mu_i$  according to

$$\mu_i' = b^{y_i} \mu_i, \quad (4.7)$$

near the fixed point of the RG. The coupling constant  $\mu_i$  is called relevant for  $y_i > 0$ , irrelevant for  $y_i < 0$  and marginal for  $y_i = 0$ . This implies that the fixed point values for all irrelevant coupling constants is zero.

By transforming the dipolar interaction into the wave-vector space and expanding it around  $q=0$  one finds three kinds of couplings [see Eq. (2.3)]: (i) the long-range dipolar coupling  $g(q^\alpha q^\beta)/q^2$ , (ii) the short-range "pseudodipolar" coupling  $hq^\alpha q^\beta$ , and (iii) the cubic term  $f(q^\alpha)^2 \delta^{\alpha\beta}$ . For the dipolar coupling constant  $g$  the RG transformation gives  $g' = b^{2-\eta} g$ ; i.e.,  $g$  is relevant. The only fixed points are  $g^* = 0$  and  $g^* = \infty$ . For  $g=0$  the pseudodipolar interaction transforms according to  $h' = b^{\lambda_h} h$  with  $\lambda_h < 0$ . Thus  $h$  is an irrelevant variable. For  $g \neq 0$ ,  $h$  becomes negligible with respect to  $g$  after a few iterations.<sup>52</sup> Similarly to  $h$ ,  $f$  also turns out to be irrelevant.<sup>53</sup>

Let us now consider the structure of the MC equations, if such irrelevant terms are retained in the Hamiltonian. For simplicity let us exemplify the main features for the pseudodipolar interaction

$$hq^\alpha q^\beta S^\alpha(\mathbf{q}) S^\beta(-\mathbf{q}),$$

which may also result from some average over the spin-orbit interaction in itinerant ferromagnets.<sup>54</sup> Then, in the equations of motion,<sup>26,27</sup>  $g$  has to be replaced by  $g + hk^2$  and the term

$$-J \int \frac{d^3k}{(2\pi)^3} \frac{1}{k} h k^2 \frac{1}{2} \frac{k_2 q}{|\mathbf{q}-\mathbf{k}|} \{S_{\mathbf{q}-\mathbf{k}}^L, S_{\mathbf{k}}^L\} \quad (4.8)$$

has to be added to the right-hand side of the equation of motion for the transverse spin components. By a simple extension of our previous calculation the vertex functions are modified according to

$$\hat{\delta}_{\beta\beta}^\alpha = \left[ 2\eta^2 \delta^{\alpha,L} + (1-\eta^2) \left[ \delta^{\beta,T} + \frac{1}{2\rho_-^2} \right] \times (1 + h \delta^{\beta,L})^2 \delta^{\alpha,T} \right] (\rho\eta - \frac{1}{2})^2, \quad (4.9a)$$

$$\hat{\delta}_{LT}^\alpha = \left[ 2(1-\eta^2 \delta^{\alpha,L}) - (1-\eta^2) \left[ 1 + \frac{1}{\rho_-^2} \right] \delta^{\alpha,T} \right] \times \left[ \rho\eta - \frac{1}{2} + \frac{y^2}{2} + \frac{h}{2} \rho^2 \right]^2. \quad (4.9b)$$

Since the pseudodipolar interaction enters the vertex functions as  $h^2 \rho^4$ , its contribution to the linewidth will come mainly from the zone boundary. However, the Hamiltonian (2.1) was obtained by an expansion with respect to  $q$ , which will overestimate the zone-boundary contributions. If one nevertheless would solve the MC equations with the vertex functions (4.9a) and (4.9b), which is trivial to do, the influence of the pseudodipolar interaction on the linewidth will be overestimated. For a proper treatment of irrelevant terms one has to know the correct Hamiltonian over the whole Brillouin zone.

Qualitatively speaking, any static irrelevant term pro-

viding an additional relaxation mechanism gives an additive contribution to the linewidth, which is noticeable as one leaves the critical region. A thorough microscopic analysis of those interactions by RG or within MC theory is meaningful only on the basis of the complete Hamiltonian over the whole Brillouin zone. In the absence of such a Hamiltonian it is much more sensible and reliable to incorporate these terms globally by a van Hove term as in Eq. (4.3).

## V. SUMMARY AND CONCLUSIONS

In this paper we have analyzed the mode-coupling theory of real ferromagnets including the short-range exchange and the dipolar interaction. In order to study the line-shape crossover the full mode-coupling equations without the Lorentzian approximation had been solved.

By incorporating the linewidth crossover in the time scale we have found that close to  $T_c$  the transverse Kubo function versus the scaled time variable  $\tau_T$  shows a pronounced shape crossover from a nearly Gaussian shape (with small damped oscillations at larger times) to an exponential shape by passing from wave vectors larger than  $q_D$  to smaller wave vectors. The line-shape crossover starts in the vicinity of the dipolar wave vector  $q_D$  in contrast to the linewidth crossover, which starts at a wave vector almost 1 order of magnitude smaller. At these temperatures the shape of the longitudinal Kubo function versus the scaled time variable  $\tau_L$  is Gaussian for small times and contains damped oscillations at larger times. Passing to smaller wave vectors the minima of the oscillations are shifted to smaller times.

The situation is quite different for temperatures well separated from the critical temperature. Then the shape for the longitudinal and transverse Kubo function is nearly the same and the shape crossover is much less pronounced. Even for wave vectors much smaller than the dipolar wave vector the shape resembles a Gaussian more at small times. Since the influence of the dipolar interaction on the critical dynamics becomes weaker as the temperature is increased, this is exactly what one would have expected from heuristic arguments.

The half-widths obtained by the complete mode-coupling theory are very similar to what one finds by the Lorentzian approximation. At small wave vectors only the nonuniversal frequency scale is modified. This is very reassuring since most of the previous applications of the theory to neutron scattering, electron-spin-resonance, magnetic relaxation, and hyperfine interaction experiments have been based on the Lorentzian approxima-

tion.<sup>26,27</sup>

In the present paper the main emphasis is put on the comparison with neutron scattering experiments. It is gratifying that the present theory<sup>37</sup> reproduces the exponential decay of the shape function determined by spin-echo experiments.<sup>15</sup>

A second issue is the peak positions in constant-energy scans which do not follow the isotropic scaling law. The presence of the second length scale  $q_D$  besides the correlation length  $\xi$ , led to a generalized scaling law for the peak position. Because of the dipolar interaction the order parameter is not conserved and thus the structure function  $S^T(\mathbf{q}, \omega)$  is nonzero at  $q=0$ . For  $T=T_c$ ,  $S^T(0, \omega)$  is proportional to  $1/\omega^2$ , which results in a strong increase of  $S^T(0, \omega)$  at small frequencies. The competition of this increase with the local maximum at finite  $q$  finally leads to a steep drop off of the scaled peak positions at small frequencies.

The preliminary comparison of our theoretical results with spin-echo measurements of Mezei on Fe gives a reasonable quantitative agreement of theory and experiment for temperatures close to the Curie temperature. Probably the agreement can be improved taking into account static crossover effects and by reanalyzing the experimental data with the known theoretical shape functions. For temperatures more separated from  $T_c$  larger discrepancies were found. They may be attributed to the van Hove background terms. Their influence has been analyzed in the previous section. The van Hove terms lead to an increase of the linewidth as one leaves the critical temperature. By approaching the critical temperature the linewidth corrections due to the van Hove terms become negligibly small.

With these theoretical results at hand, available experiments could be analyzed more accurately. In addition, some of the predictions as, for instance, the behavior of the longitudinal correlation function, could be tested.

*Note added in proof.* The shape crossover was also considered in two recent papers by Aberger and Folk [Physica B **156&157**, 229 (1989); J. Phys. (Paris) Colloq. C **8**, 1567 (1988)]. A review of the dipolar crossover has been given by Frey and Schwabl [J. Phys. (Paris) Colloq. C **8**, 1531 (1988)] and Schwabl [J. Appl. Phys. **64**, 5867 (1988)].

## ACKNOWLEDGMENTS

This work has been supported by the German Federal Ministry for Research and Technology (BMFT) under Contract No. 03-SC1TUM-0.

<sup>1</sup>R. C. Reno and C. Hohenemser, *Magnetism and Magnetic Materials (Chicago, 1971)*, Proceedings of the 17th Annual Conference on Magnetism and Magnetic Materials, AIP Conf. Proc. No. 5, edited by D. C. Graham and J. J. Rhyne (AIP, New York, 1972).

<sup>2</sup>A. M. Gottlieb and C. Hohenemser, Phys. Rev. Lett. **31**, 1222 (1973).

<sup>3</sup>C. Hohenemser, L. Chow, and R. M. Suter, Phys. Rev. B **26**, 5056 (1982); Phys. Rev. Lett. **45**, 908 (1980).

<sup>4</sup>C. Hohenemser, N. Rosov, and A. Kleinhammes, Proceedings of the International Conference on Nuclear Methods in Magnetism, München, 1988 [Hyp. Int. (to be published)].

<sup>5</sup>J. Kötzler, G. Kamleiter, and G. Weber, J. Phys. C **9**, L361 (1976).

<sup>6</sup>J. Kötzler, W. Scheithe, R. Blickhan, and E. Kaldis, Solid State Commun. **26**, 641 (1978).

<sup>7</sup>J. Kötzler and H. von Philipsborn, Phys. Rev. Lett. **40**, 790 (1978).

- <sup>8</sup>J. Kötzer and W. Scheithe, *J. Magn. Magn. Mater.* **9**, 4 (1978).
- <sup>9</sup>R. A. Dunlap and A. M. Gottlieb, *Phys. Rev. B* **22**, 3422 (1980).
- <sup>10</sup>J. Kötzer, *Phys. Rev. B* **38**, 12 027 (1988).
- <sup>11</sup>M. F. Collins, V. J. Minkiewicz, R. Nathans, L. Passell, and G. Shirane, *Phys. Rev.* **179**, 417 (1969).
- <sup>12</sup>O. W. Dietrich, J. Als-Nielsen, and L. Passell, *Phys. Rev. B* **14**, 4923 (1976).
- <sup>13</sup>F. Mezei, *Phys. Rev. Lett.* **49**, 1096 (1982).
- <sup>14</sup>F. Mezei, *J. Magn. Magn. Mater.* **45**, 67 (1984).
- <sup>15</sup>F. Mezei, *Physica B* **136**, 417 (1986).
- <sup>16</sup>F. Mezei, in *Magnetic Excitations and Fluctuations*, edited by U. Balucani, S. W. Lovesey, M. Rasetti, and V. Tognetti, Vol. II of *Springer Proceedings in Physics* (Springer-Verlag, Berlin, 1987).
- <sup>17</sup>F. Mezei, Proceedings of the International Conference on Magnetism, Paris, 1988 [*J. Phys. Colloq.* **C8**, 1537 (1988)].
- <sup>18</sup>J. P. Wicksted, P. Böni, and G. Shirane, *Phys. Rev. B* **30**, 3655 (1984).
- <sup>19</sup>P. Böni and G. Shirane, *Phys. Rev. B* **33**, 3012 (1986).
- <sup>20</sup>P. Böni, M. E. Chen, and G. Shirane, *Phys. Rev. B* **35**, 8449 (1987).
- <sup>21</sup>P. Böni, G. Shirane, H. G. Bohn, and W. Zinn, *J. Appl. Phys.* **61**, 8 (1987).
- <sup>22</sup>P. Böni, G. Shirane, H. G. Bohn, and W. Zinn, *J. Appl. Phys.* **63**, 3089 (1988).
- <sup>23</sup>P. Resibois and C. Piette, *Phys. Rev. Lett.* **24**, 514 (1970).
- <sup>24</sup>S. Ma and G. F. Mazenko, *Phys. Rev. B* **11**, 4077 (1975).
- <sup>25</sup>H. Iro, *Z. Phys. B* **68**, 485 (1987).
- <sup>26</sup>E. Frey and F. Schwabl, *Phys. Lett. A* **123**, 49 (1987); E. Frey, Diploma thesis, Technische Universität München, 1986 (unpublished).
- <sup>27</sup>E. Frey and F. Schwabl, *Z. Phys. B* **71**, 355 (1988).
- <sup>28</sup>F. Wegner, *Z. Phys.* **216**, 433 (1968).
- <sup>29</sup>J. Hubbard, *J. Phys. C* **4**, 53 (1971).
- <sup>30</sup>A. Cuccoli, V. Tognetti, S. W. Lovesey, and R. Vaia, *Phys. Lett. A* **131**, 57 (1988).
- <sup>31</sup>A. Cuccoli, V. Tognetti, and S. W. Lovesey, *Phys. Rev. B* **39**, 2619 (1989).
- <sup>32</sup>V. Dohm, *Solid State Commun.* **20**, 657 (1976).
- <sup>33</sup>J. K. Bhattacharjee and R. A. Ferrell, *Phys. Rev. B* **24**, 6480 (1981).
- <sup>34</sup>R. Folk and H. Iro, *Phys. Rev. B* **32**, 1880 (1985).
- <sup>35</sup>S. W. Lovesey and R. D. Williams, *J. Phys. C* **19**, L253 (1986).
- <sup>36</sup>U. Balucani, M. G. Pini, P. Carra, S. W. Lovesey, and V. Tognetti, *J. Phys. C* **20**, 3953 (1987).
- <sup>37</sup>E. Frey, F. Schwabl, and S. Thoma, *Phys. Lett. A* **129**, 343 (1988).
- <sup>38</sup>R. Folk and H. Iro, *Phys. Rev. B* **34**, 6571 (1986).
- <sup>39</sup>A. Aharony and M. E. Fisher, *Phys. Rev. B* **8**, 3323 (1973).
- <sup>40</sup>A. D. Bruce, J. M. Kosterlitz, and D. R. Nelson, *J. Phys. C* **9**, 825 (1976).
- <sup>41</sup>E. Frey and F. Schwabl, Proceedings of the International Conference on Magnetism, Paris, 1988 [*J. Phys. Colloq.* **C8**, 4569 (1988)].
- <sup>42</sup>F. Mezei (private communication).
- <sup>43</sup>C. Aberger and R. Folk, *Phys. Rev. B* **38**, 7207 (1988).
- <sup>44</sup>C. Aberger and R. Folk, *Phys. Rev. B* **38**, 6693 (1988).
- <sup>45</sup>M. Manson, *J. Phys. C* **7**, 4073 (1974).
- <sup>46</sup>K. Kawasaki, *J. Phys. A* **6**, 1289 (1973).
- <sup>47</sup>H. Mori, *Prog. Theor. Phys.* **33**, 423 (1965).
- <sup>48</sup>K. Kawasaki, in *Phase Transitions and Critical Phenomena*, edited by C. Domb and M. S. Green (Academic, New York, 1976), Vol. 5a.
- <sup>49</sup>K. Kawasaki, *Ann. Phys. (N.Y.)* **61**, 1 (1970).
- <sup>50</sup>E. Frey and F. Schwabl, Proceedings of the International Conference on Nuclear Methods in Magnetism, München, 1988 [*Hyp. Int.* (to be published)].
- <sup>51</sup>K. G. Wilson and J. Kogut, *Phys. Rep.* **12C**, 76 (1974).
- <sup>52</sup>A. Aharony, in *Phase Transitions and Critical Phenomena*, edited by C. Domb and M. S. Green (Academic, New York, 1976), Vol. 6.
- <sup>53</sup>A. Aharony, *Phys. Rev. B* **8**, 3349 (1973).
- <sup>54</sup>J. H. van Vleck, *Phys. Rev.* **52**, 1137 (1937).